3D Human Gait Reconstruction and Monitoring Using Body-Worn Inertial Sensors and Kinematic Modeling

Amin Ahmadi, *Member, IEEE*, François Destelle, Luis Unzueta, *Member, IEEE*, David S. Monaghan, *Member, IEEE*, Maria Teresa Linaza, Kieran Moran, and Noel E. O'Connor, *Member, IEEE*

***Abstract*— In this paper, we present a novel low-cost computationally efficient method to accurately assess human gait by monitoring the 3D trajectory of the lower limb, both left and right legs outside the lab in any unconstrained environment. Our method utilizes a network of miniaturized wireless inertial sensors, coupled with a suite of real-time analysis algorithms and can operate in any unconstrained environment. First, we adopt a modified computationally efficient, highly accurate, and near real-time gradient descent algorithm to compute the direction of the gyroscope measurement error as a quaternion derivative in order to obtain the 3D orientation of each of the six segments. Second, by utilizing the foot sensor, we successfully detect the stance phase of the human gait cycle, which allows us to obtain drift-free velocity and the 3D position of the left and right feet during functional phases of a gait cycle. Third, by setting the foot segment as the root node we calculate the 3D orientation and position of the other two segments as well as the left and right ankle, knee, and hip joints. We then employ a customized kinematic model adjustment technique to ensure that the motion is coherent with human biomechanical behavior of the leg. Pearson's correlation coefficient (r) and significant difference test results (P) were used to quantify the relationship between the calculated and measured movements for all joints in the sagittal plane. The correlation between the calculated and the reference was found to have similar trends for all six joints ($r > 0.94$, $p < 0.005$).**

***Index Terms*— Kinematic model, wearable inertial sensors, 3D trajectory, human gait.**

I. Introduction

THE advancement of sensor manufacturing, or computer microminiaturisation, in recent times is a continuing driver of research into a wide variety of scientific fields including the Internet-of-Things. The Internet-of-Things is an area where a network of interconnected sensors, electronics and software can transfer data and has mainly come about through the availability of new low-cost sensors that may be embedded into everyday items. This increasing availability of low-cost sensors is also having a major influence on the field of biomechanical gait analysis [1], [2].

We can define gait analysis as the systematic study of human walking or running (locomotion) [3]. An accurate gait analysis is extremely useful for athletes, both professional and amateur, and also for the general population in order to assess and treat individuals with (pathological) conditions that affect their ability to walk and their entire muscular skeletal system [4]–[6]. Traditionally, gait analysis involved a human observer monitoring a subject but this was subsequently augmented with video recording, where the recording could be reviewed in slow motion to allow a more accurate assessment of the gait cycle. This approach of qualitative analysis is still widely used today. However, this method is labour intensive, requires a highly trained sports-scientist or clinician, and is not as accurate as methods that quantify movement.

The capture and analysis of human movements (e.g. walking, jumping and running) is common in a number of domains, including: sport science, musculoskeletal injury management, rehabilitation, clinical biomechanics and the gaming/movie industry. The analysis of joint/body segment position, angles and angular velocities, requires highly accurate motion capture or MoCap. Real-time MoCap technology used alongside video analysis can produce more accurate data and allow for a more in depth analysis of gait [3]. This can provide the clinician with a large amount of quantitative biomechanical data, important in assessing joint orientation, acceleration and relative position.

MoCap is a field of science that primarily deals with the recording, reconstruction and analysis of motion, and is a well-studied and broad area of research [7]. MopCap can be segmented into two separate camps: (1) Marker-based motion capture systems, (2) Markerless-based systems [8]. Marker based Vicon MoCap offers excellent results but carries a restrictively high price tag and requires complex post-processing, leaving it out of reach for the general public. For this reason, significant research is being performed into the area of low-cost alternatives [9], [10], using either markerless based methods such computer vision [1], [11]–[13] based analysis, or body worn devices [2], [14]–[16], or by using depth cameras like the Microsoft Kinect [17], [18]. How-

Manuscript received February 29, 2016; revised June 19, 2016; accepted July 8, 2016. Date of publication July 19, 2016; date of current version November 17, 2016. This work was supported by the European Community's Seventh Framework Programs (FP7/2013-2016) through the REPLAY Project under Grant ICT-2011-8.2.601170. This paper was presented at the IEEE SENSORS 2015 Conference, Busan, South Korea. The associate editor coordinating the review of this paper and approving it for publication was Prof. Gijs Krijnen.

A. Ahmadi, F. Destelle, D. S. Monaghan, and K. Moran are with the Insight Centre for Data Analytics, Dublin City University, Dublin 9 Dublin, Ireland (e-mail: ahmadi.amin@gmail.com; francois.destelle@dcu.ie; david.monaghan@dcu.ie; kieran.moran@dcu.ie).

L. Unzueta and M. Teresa Linaza are with Vicomtech-IK4, Donostia 20009, Spain (e-mail: lunzueta@vicomtech.org; mtlinaza@vicomtech.org).

N. E. O'Connor is with the School of Electronic Engineering, Dublin City University, Glanevin, Dublin 9 Dublin, Ireland (e-mail: noel.oconnor@dcu.ie).

Digital Object Identifier 10.1109/JSEN.2016.2593011

ever, many of these systems suffer from tracking errors due to marker occlusions and inaccuracies in transverse plane rotations.

Inertial Measurement Units (IMU) potentially offer an accurate MoCap alternative [19], [20] and these kinds of sensors are now widely available. Previous research [20] carried out by the authors investigated a low-cost platform that utilises three readily available IMU sensors together with advanced analysis algorithms for detecting the stance phase of the gait cycle, multiple IMU calibration and inverse kinematics. This allows for the reduction in the integration drift error of the velocity in the IMU system and enabling the creation of an accurate 3D gait analysis platform for the lower limbs.

Among the wide variety of possible options, inertial sensors offer the most attractive capabilities, particularly in light of recent advancements in MicroElectroMechanical Systems technology resulting in cheap unobtrusive (small) sensors. It has been shown how body limb positions can be directly inferred from wearable accelerometer data streams [21]. Combining an accelerometer with a magnetometer and a gyroscope into a single Wireless Inertial Measurement Unit (WIMU) device, allows sensor yaw to be determined and can help increase robustness. WIMUs have been incorporated into commercial products, such as XSens [22]. However, they are still prone to drift in accuracy over time, which constitutes a common limitation of inertial sensing. Incorporating further sensors, such as ultrasonic time-of-flight devices, on the body can reduce the negative impact of this drift [23]. In addition, they require low power, are light-weight, and offer high sample rates. However, many of these systems are prone to drift in accuracy over time, a common limitation of inertial sensors, making them susceptible to orientation and position errors. This is extremely important if there is to be a move away from laboratory-based assessment of gait, which lacks ecological validity due to the low number of steps being analysed (possibly <5) under very artificial and controlled conditions, to a more free-living assessment [24]; which is in line with the concept of the Internet-of-Things. Extended assessment of gait (over tens of minutes or even hours) during free-living, especially if longitudinal in nature, may provide a yet to be realized insight into neural-musculoskeletal injuries and cognitive decline. Furthermore, commercially available IMU MoCap solution are still relatively high in price, approx. 50K.

Unfortunately, the more accurate motion capture systems tend to be expensive, whether camera based (e.g. Vicon) or inertia sensor based (e.g. XSens). This places highly accurate motion capture outside the reach of most users. During the last few years, a number of different methodologies have been proposed to address this issue. The majority of these approaches are based upon fusing data received from different cheap sensor modalities (e.g. fusion of Kinect & wearables) [25], [26] to provide inexpensive yet accurate systems.

In this paper we present a truly low-cost platform that is comprised of 7 low-cost, readily available IMU sensors together with advanced analysis algorithms, multiple IMU automatic calibration algorithms and inverse kinematics analysis. Furthermore, our system contains stance-phase detection, which reduces the integration drift error of the velocity in the IMUs. We compare our results to a gold standard marker based MoCap gait analysis system (Vicon, UK).

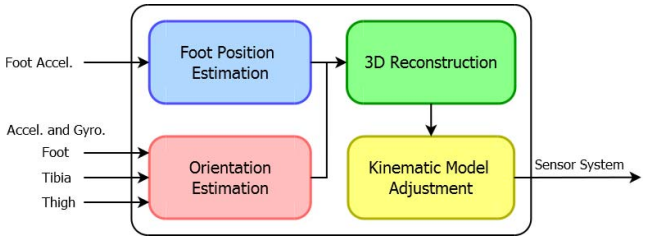

Fig. 1. The main components of the proposed framework.

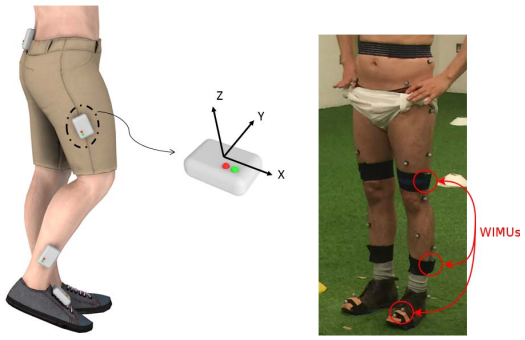

Fig. 2. Placement of wireless inertial sensor units and Vicon markers.

This paper represents a substantive extension to our previous experimental work [20]. In particular, it extends our work by increasing the number of sensors from 3 to 7 and enhancing the model to generate the entire lower body (i.e. both left and right legs).

II. Proposed Framework

The main components of our framework are illustrated in Fig. 1. It consists of four main components, which are: (1) orientation estimation; (2) foot position estimation; (3) 3D reconstruction; and (4) kinematic model adjustment. Each component is presented and discussed in Section III.

III. Methodology

A. Experimental Setup

Data was collected using seven wearable inertial sensors (x-IMU, x-io Technologies, UK) positioned on the participants' feet, tibias, thighs and pelvis, as seen in Fig. 2. Each inertial sensor-based device contained one tri-axis accelerometer and one tri-axis gyroscope. x, y and z axes of the 3D accelerometer and 3D gyroscope attached on a right thigh is depicted in Fig. 2. The x-axes were aligned with the longitudinal axes of the body segments. An internal SD card was used to store data from each sensor at 256Hz. A physical event (5 stiff jumps) was used to temporally synchronize the sensors at the start and end of the walking trial. The initial rise in the fifth peak was used for synchronisation. Pilot work demonstrated an accuracy of $0.010 \pm 0.002ms$ $(mean \pm std)$.

In addition, the Vicon motion-capturing system using the standard Plug-in Gait model was used to validate the results, and optical markers were attached on the lower body of the participant. The placement of markers, with respect to the

standard Plug-in Gait model, is shown in Fig. 2. Twelve cameras were used to record the data at 200 frames per second. Once the inertial sensors and the Vicon markers were attached on the subject, and he performed the stiff jumps, he was then asked to pause for 3 seconds with his legs in parallel and aligned with the y-axis of the Vicon coordinate system. Next, the subject was asked to start walking freely on a straight line and then ascending/descending the steps inside the Vicon capturing volume. Six trials were captured to be used to validate the outcome of our system. The experimental procedures involving human subjects described in this paper were approved by the Institutional Review Board.

B. Orientation Estimation

Although there are different technologies to monitor human body orientation, wearable inertial sensors have the advantage of being self-contained in a way that measurement is independent of motion and environment. It is feasible to measure accurate orientation in three-dimensional space by utilizing tri-axial accelerometers, gyroscopes and a proper filter. In this paper, we employed a gradient descent optimization algorithm, which has been shown to provide effective performance at low computational expense over an extended period of time [27]. The algorithm [27] employs a quaternion representation of orientation and is not subject to the problematic singularities associated with Euler angles. A tri-axis gyroscope will measure the angular rate about the x, y and z axes of the sensor frame, termed ω_x , ω_y and ω_z respectively. If these parameters are arranged into the vector S_ω defined below, the quaternion derivative describing rate of change of the earth frame relative to the sensor frame ${}^S_E q$ can be calculated using the following equation. The $\otimes$ operate denotes a quaternion product and the accent ^denotes a normalised vector of unit length.

$$\begin{cases} S_\omega = [0, \omega_x, \omega_y, \omega_z] \\ {}^S_E\dot{q} = \frac{1}{2}{}^S_E\hat{q} \otimes S_\omega \end{cases} \tag{1}$$

The estimated orientation rate is defined in the following equations [27]:

$$\begin{cases} {}^S_E q_t = {}^S_E\, q_{t-1} + {}^S_E\, \dot{q}_t \Delta t \\ {}^S_E\dot{q}_t = {}^S_E\, \dot{q}_{\omega,t} - \beta \frac{\nabla f}{||\nabla f||} \end{cases} \tag{2}$$

where

$$\begin{cases} \nabla f({}^S_E q, E_g, S_a) = J^T({}^S_E q, E_g) f({}^S_E q E_g, S_a) \\ S_a = [0, a_x, a_y, a_z] \\ E_g = [0, 0, 0, 1] \end{cases} \tag{3}$$

In this formulation, ${}^S_E q_t$ and ${}^S_E q_{t-1}$ are the orientation of the Earth frame relative to the sensor frame at time t and $t-1$ respectively. ${}^S_E\dot{q}_{\omega,t}$ is the rate of change of orientation measured by the gyroscopes. S_a is the acceleration in the x, y and z axes of the sensor frame, termed a_x, a_y, a_z respectively. This acceleration vector is generated using the data obtained directly from the 3D accelerometers and hence contain both static and dynamic acceleration in the 3D space. The algorithm calculates the orientation ${}^S_E q_t$ by integrating the estimated rate of change of orientation measured by the gyroscope. Then gyroscope measurement error, β, was removed in a direction based on accelerometer measurements. We chose the value of β to be high enough to minimize errors associated with integral drift but also low enough to avoid noise due to large steps of gradient descent iterations. This algorithm uses a gradient descent optimization technique to measure only one solution for the sensor orientation by knowing the direction of the gravity in the Earth frame. f is the objective function and J is its Jacobean (J^T is transpose of J) and they are defined by the following equations:

$$f(q, S_a) = \begin{bmatrix} 2(q_2q_4 - q_1q_3) - a_x \\ 2(q_1q_2 + q_3q_4) - a_y \\ 2(0.5 - q_2^2 - q_3^2) - a_z \end{bmatrix} \tag{4}$$

$$J(q) = \begin{bmatrix} -2q_3 & 2q_4 & -2q_1 & 2q_2 \\ 2q_2 & 2q_1 & 2q_4 & 2q_3 \\ 0 & -4q_2 & -4q_3 & 0 \end{bmatrix} \tag{5}$$

This algorithm is capable of computing an error based on an analytically derived Jacobean that results in a significant reduction in the computation load [27], [28]. This technique was developed to estimate the sensor orientation with respect to the earth frame during the entire gait cycle. The static and dynamic RMS errors of the orientation estimation algorithm are $< 0.8°$ and $< 1.7°$ respectively, thus achieving an accuracy level matching that of the Kalman based algorithm [27], [28].

C. Position Estimation

Human gait motion is a cyclic motion consisting of two main phases, the stance phase where the foot is in contact with the ground and the swing phase where the foot is traversing from one stance phase to the next. With precisely accurate IMUs a double integration of the acceleration data yields accurate 3D position. However, IMUs have small errors in acceleration and thus the position estimates based upon a double integration technique can only be valid for a short period of time as these errors are accumulative and lead to 3D position drift. To overcome such a problem and avoid this accumulated error, we detect the stance and swing phases automatically during the entire gait cycle. Therefore, the error produced when velocity and position estimation are calculated for one cycle does not accumulate and influence those on consecutive gait cycles.

The overview of the 3D foot position estimation is illustrated in Fig. 4. This method obtains accurate 3D position while using the double integration technique by correcting the drift error at each stance phase [28]–[31]. During each gait cycle, 3D orientation, velocity, and trajectory of foot were estimated from inertial signals. Practically, this involves the temporal detection of cycles, the knowledge of initial conditions of position and orientation, the gravity cancellation of measured acceleration, and the de-drifted integration of g-free acceleration. Moreover, kinematics measured by sensors in local frame should be expressed in global frame to be compared with reference using the following equation.

$${}^E_S q = {}^S_E\, q \otimes S_a \otimes {}^S_E\, \overline{q} \tag{6}$$

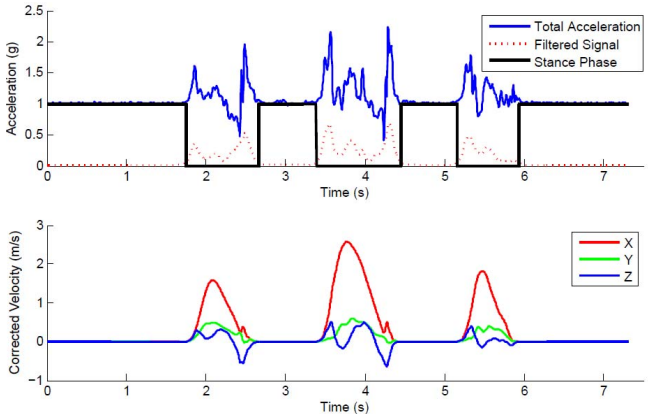

Fig. 3. Total acceleration along with filtered signals and stance phases (bottom) as well as corrected velocity (top) are illustrated.

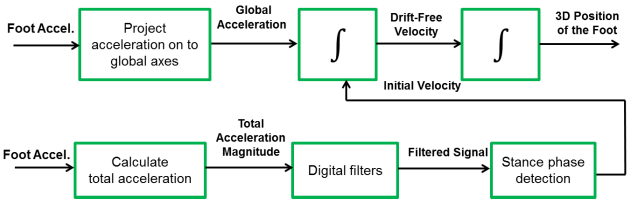

Fig. 4. Overview of the foot position estimation process.

In this notation, $\otimes$ denotes the quaternion multiplication, ${}^{E}_{S}q$ is the orientation of the sensor frame relative to the earth frame and $\overline{q}$ denotes the quaternion conjugate. Temporal detection of gait cycles was done using absolute value of the total acceleration of foot to identify stance phase using the sensor attached on the foot. For each stance phase, foot-flat was defined as the continuous period where total acceleration norm was below certain threshold (it is non-zero but it is lower than an experimentally obtained threshold). Initial conditions were updated for each cycle at each stance phase, where the foot was considered motion-less.

It is necessary to filter the signals in order to eliminate small fluctuations. Butterworth filters are one of the most commonly used digital filters in motion analysis. We opted for digital Butterworth filters as they are fast, simple to use and characterized by a magnitude response that is maximally flat in the passband and monotonic overall. These are all required features to ensure a system generates accurate results in near real-time. We utilized a first order high-pass digital Butterworth filter (cutoff frequency $=$ 0.001Hz) and then a first order low-pass digital Butterworth filter (cutoff frequency $=$ 5Hz) to remove noise and hence to accurately identify the stance phase throughout the entire gait cycle. The total acceleration signal along with the filtered signal and stance phases as well as corrected velocity during stance phase are depicted in Fig.3.

Once the stance phase is successfully detected, the velocity can be corrected during that phase (i.e. initial velocity is set to zero) and subsequently the 3D position of the foot during the swing phase can be calculated [32]. Calculated 3D position of the foot sensor with respect to the global frame during walking and ascending steps are illustrated in Fig. 5.

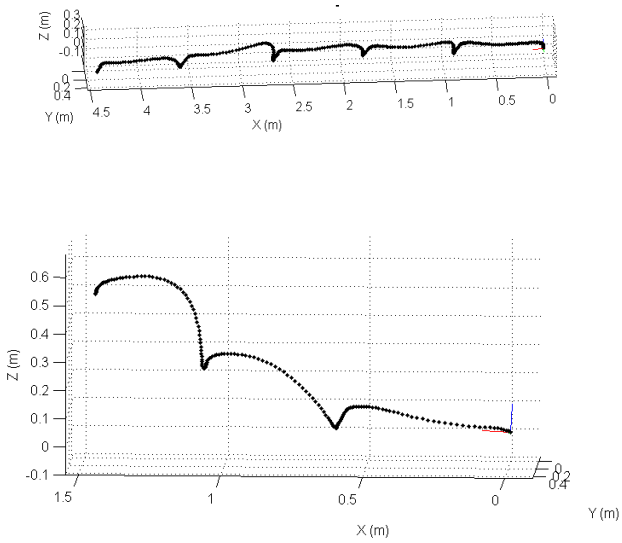

Fig. 5. Calculated 3D position of the foot sensor with respect to the global frame during walking (top) and ascending steps (bottom) are illustrated.

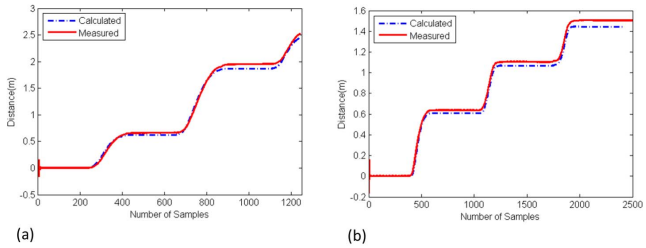

Fig. 6. The calculated and measured foot position in a sagittal plane (longitudinal axis) traversed by a subject (a) walking on a straight line and (b) ascending stairs are shown.

In addition, Fig. 6 illustrates a similar trend and close relationship between the foot trajectory obtained from the sensor attached on the foot with that measured using the Vicon system (reference) in the sagittal plane (longitudinal axis) while subject is walking on a straight line and ascending stairs.

D. 3D Reconstruction

We aim to animate a skeletal model only from the estimation of the ankle position and the changes in local orientation from each sensor. In order to synthesize a skeletal model of the subject's bones, taking into account that we only estimate the position of an ankle we first need to create a fixed skeleton of reference.

This skeleton is modelled by a stick figure, see Fig. 8(a). In our current implementation, we are using both legs and we added another sensor on the lower-back of the subject, see Fig. 7. This additional sensor added to our method allows the reconstruction of another bone, showing it's flexibility, and it permits to compute the hips 3D joint angles as a difference of two 3D segment angles. In the following, we will describe the 3D reconstruction of one leg, as the extension to another limbs follow the same technical scheme and as such is straightforward. The skeleton of reference assumes a perfect standing pose at the beginning: the legs are vertical and the

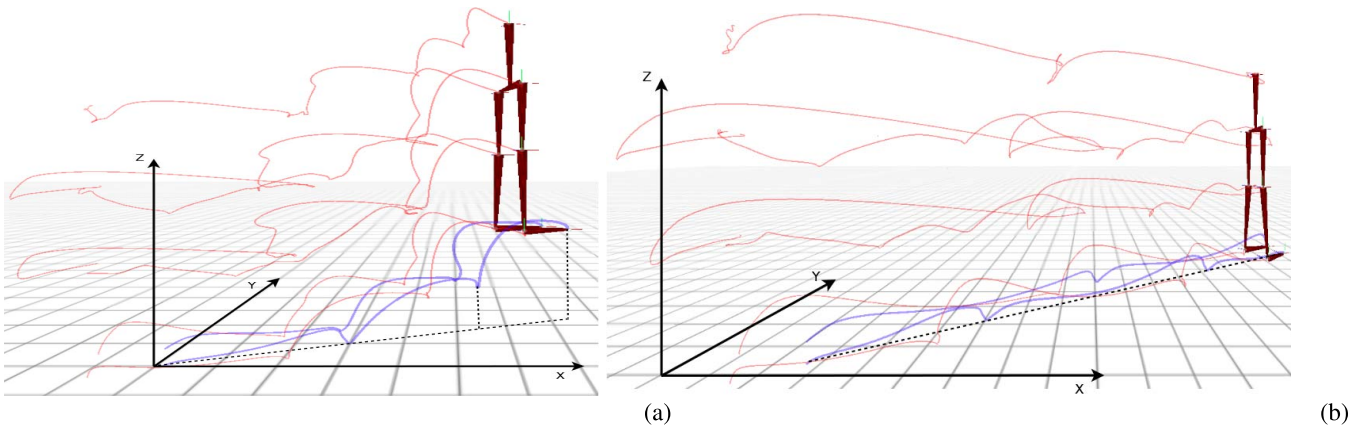

Fig. 7. Reconstruction of both legs and the lower back additional bone showing that our method can potentially be extended to reconstruct upper body as well. (a) The subject is walking and then ascending 2 stairs, (b) the subject is only walking 3 regular steps inside. The blue lines depict the estimated position of the foot (see Fig. 5) while the red lines depict the trajectory of each joint over time.

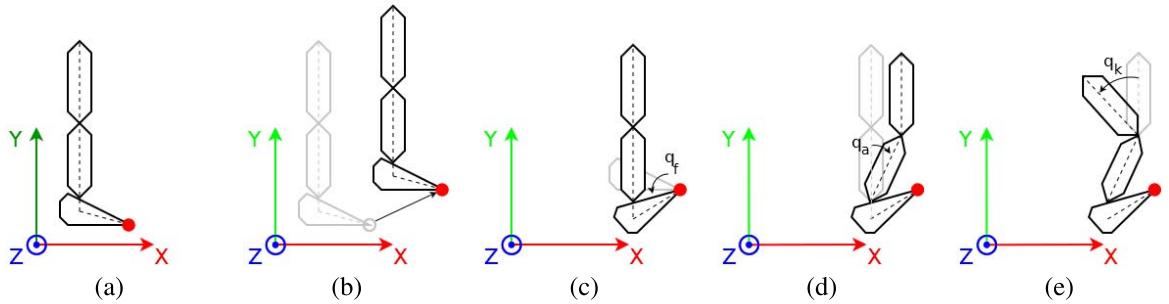

Fig. 8. Diagram of the 3D gait reconstruction method. (a) We start from the first frame of the sequence, the first one being our fixed reference. (b) All the joints are translated relative to our evaluation of the foot displacement. (c) We then rotate the foot segment relative to the foot sensor orientation. In a hierarchical manner, we then rotate the tibia (d) inducing a new thigh position. (e) Finally, we rotate the thigh segment with respect to the orientation of the thigh sensor, inducing the final hip joint position.

feet are pointing in front of the model. Relative to our specific sensor placement (see Fig. 2), the front direction is aligned with the direction $X : \{1, 0, 0\}$ of our global coordinates system. This consideration is useful in order to facilitate the calibration of several coordinate systems, e.g. Vicon or Kinect motion capture systems. Considering one leg, this geometrical reference is then animated using only the position of the foot sensor and the rotational estimations of the three sensors in a hierarchical manner as depicted in Fig. 8(b-e). This 3D reconstruction approach uses a very similar method presented in [25], using here the lower part of the subject's body only. In this previous work, we compared the precision of the joint angle reconstruction against the motion capture standard Vicon, it achieves a mean RMS accuracy error of 7 degrees and a normalized cross correlation (NCC) of 8.3.

1) Initial Skeleton of Reference: In this section, the reconstruction of one leg (right leg) is explained. The same technique can be utilized to reconstruct the other limb. We consider for one leg the set of joints positions for a sequence frame t as $p^t : \{p_f^t, p_a^t, p_k^t, p_h^t\}$, respectively the position of the foot, the ankle, the knee and the hip. The virtual ankle position can be calculated using the computed 3D foot position described in section III-C. Let the initial position of each skeleton joint to be $p_0 : \{p_f^0, p_a^0, p_k^0, p_h^0\}$. Also the length of the foot l_f, tibia l_k and thigh l_t need to be accurately measured prior to reconstructing the leg in order to be able to

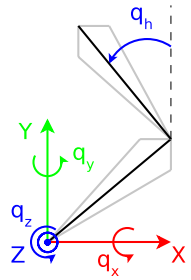

Fig. 9. A knee flexion along the direction X implies a rotation along the Z axis.

evaluate our system by comparing it to other motion capture frameworks. In our experiments, we measured the subject's segments length. $l_f = 20$cm, $l_k = 42$cm, $l_t = 35$cm and $l_s = 20$cm where l_f, l_k, l_t and l_s are the length of his foot, the displacements between his ankle and the knee, his knee and his thigh and his legs spacing, respectively. During the whole animation process, the length of each bone remains constant.

2) Calibration of the Orientation: Prior to animate the reconstructed skeleton a calibration step is required to effectively use the estimated orientations $q_t : \{q_t^f, q_t^a, q_t^k\}$, of all the sensors placed on the subject's foot, tibia and thigh. Firstly, the local coordinate systems of each sensor has to be mapped to the global coordinate system $\{X, Y, Z\}$. Secondly, as can be seen in Fig. 9, a spatial displacement of the foot along the

X axis, implying a knee flexion, does not indicate a sensor rotational variation along the same axis. This calibration step is required to ensure the consistency of each local coordinate system with respect to the global one.

3) Animation of the Reconstruction Over Time: The first step of the animation algorithm at frame t is to update the foot joint position by using the previous frame p_f^{t-1}. All the remaining joint positions are then translated from their initial positions to the new ones relative to the new ankle joint position. In the next step, the ankle position is updated utilizing the estimated 3D orientation of the foot sensor, inducing new position for all the other joints. Then the tibia segment is rotated using the estimated orientation of the tibia sensor. This results in generating new positions for the knee and hip joints. Finally the thigh segment orientation is updated using the estimated orientation of the thigh sensor and leads to the final position of the hip joint, see Fig. 8. The reconstructed skeleton is evaluated for a frame t using:

$$\begin{cases} p_a^t = p_f^t + q_f^t \otimes (\ l_f X\ ) \otimes \overline{q_f^t} \\ p_k^t = p_a^t + q_a^t \otimes (\ l_k Y\ ) \otimes \overline{q_a^t} \\ p_h^t = p_k^t + q_k^t \otimes (\ l_t Y\ ) \otimes \overline{q_k^t}, \end{cases} \tag{7}$$

In this notation, $\otimes$ denotes the quaternion multiplication, $\overline{q}$ denotes the quaternion conjugate and $X : \{1, 0, 0\}$ (left) and $Y : \{0, 1, 0\}$ (up) are oriented considering the global coordinate system of our scene. Position and trajectory of both legs (i.e. left and right feet, tibias and thighs) during multiple gait cycles are depicted in Fig. 7.

E. Kinematic Model Adjustment

Once the positions and orientations of the lower limb joints have been estimated by the sensors, it is still necessary to apply another procedure to ensure that the motion is coherent with their biomechanical behaviour, which might not occur if the sensor data is applied directly to the body joints of a kinematic model that would represent the lower limbs. Furthermore, the positional uncertainty of the sensors can lead to errors, despite the initial calibration, especially during motion. This effect can be diminished by adjusting a kinematic model to the measured data, taking into account biomechanical constraints and the level of confidence of the measured data. Thus, the final motion will be a combination of measured data and biomechanical constraints that will correct unnatural poses.

Inverse Kinematics (IK) allows to estimate the full configuration, i.e., degrees of freedom (DoF), of multi-body kinematic structures, such as the lower body limbs, having only some measured data available (normally, the end-effector positions). There are different IK strategies that could be applied. In general, IK approaches can be distinguished as: analytical [33]–[35], numerical [36]–[38] and hybrid methods [39]–[41]. Analytical methods allow to find all possible solutions based on the mechanism segment lengths, its starting posture and the rotation constraints. Compared to other strategies, lower computational cost can be obtained and good accuracy. However, they can only be used for simple mechanisms with few DoF and they are not feasible when the system is ill-posed. On the contrary, numerical methods

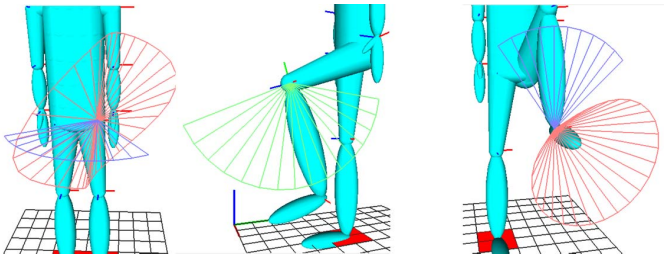

Fig. 10. Biomechanical constraints of the leg joints.

can be applied to complex mechanisms. These methods cover those that require a set of iterations to achieve a satisfactory solution. One important advantage of numerical approaches is that their results can be enhanced by enforcing priorities to arbitrate the fulfillment of conflicting constraints. Finally, hybrid methods are those that combine both analytical and numerical algorithms with the objective of taking advantage of the pros of each kind of strategy, by adopting local and global reconstruction procedures in a coherent way. In this work, we propose a hybrid method that subdivides the lower-limb kinematic model into three main substructures, i.e., pelvis, left leg and right leg, enforcing priorities according to the measured data features that are more trustworthy.

Thus, each leg has 3 DoF for the hip and ankle joints and 1 DoF for the knee, with boundaries such as those shown in Fig. 10. These complex boundaries can be obtained if the rotations are modelled using the circumduction-swing-twist parameterization proposed in [40].

The modeling of these boundaries is based on a spherical parametrization of orientations, ignoring variations in the radius direction, as the body segment has a constant size. Only the other two angles are considered; the circumduction angle θ, and swing amplitude or ψ, are considered. The range of θ goes from $-\pi$ to $+\pi$, and for each value there is a corresponding biomechanical limit of ψ. A set of n biomechanical limits are measured in the subject, such as the hips flexion, extension, abduction and adduction. Then, the rest are obtained by applying a cubic spline, with the first derivative at its starting and ending points ($\theta = -\pi$ and $\theta = \pi$, respectively) estimated as shown in Eq. 8, in order to get a smooth boundary over the entire circumduction movement.

$$\left.\frac{\partial \psi}{\partial \theta}\right|_1 = \left.\frac{\partial \psi}{\partial \theta}\right|_n = \frac{1}{2}\left(\frac{\psi_2 - \psi_1}{\theta_2 - \theta_1} + \frac{\psi_n - \psi_{n-1}}{\theta_n - \theta_{n-1}}\right). \tag{8}$$

The twist rotation needs a reference to which the current orientation is compared. This is obtained by considering the orientation of the parent joint as the neutral orientation of the current joint, and then rotating it with the θ and ψ values corresponding to the current orientation. This way the reference orientation differs from the current one only on the twist rotation.

Thus, in order to apply the IK strategy appropriately, it is necessary to prioritize some of the measured data that are more trustworthy. In this case, we give more importance to the measured positions of the pelvis and the ankles, based on experimental observations. The positions of the ankles are closer to the reality, compared to the rest of the leg joints, as they are the ones that are deduced more directly from

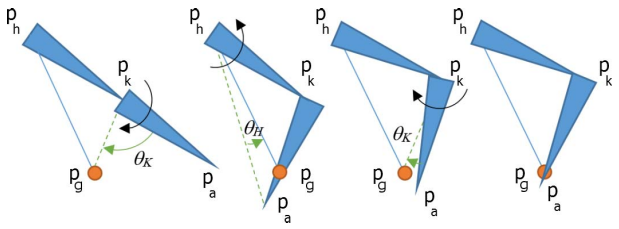

Fig. 11. A set of iterations of the CCD IK procedure applied to the leg, in order to make the ankle joint (P_a) match the measured goal (P_g).

the sensors, and hence, accumulate less error. Regarding the pelvis position, it can be deduced from the left and right leg chains and therefore, taking into account the symmetry of the mechanism, the accumulated errors can be compensated. These features are enough to adjust the kinematic model, by assuming that the person is walking in a straight line, as follows:

1) Initialize the pose, by applying the measured pelvis position to the pelvis joint.
2) Apply the Cyclic Coordinate Descent (CCD) Inverse Kinematics (IK) procedure described in [36] to adjust the hip and knee orientations, so that the ankle joint matches its measured position.
3) 3. Set the measured ankle orientation to the ankle joint of each leg.

The CCD IK procedure is fast and allows to check and correct the biomechanical configuration with respect to the modeled boundaries at each iteration, if required. Therefore, this additional procedure allows to satisfactorily infer the non-prioritized motion of the subject, preserving the biomechanical constraints. Fig. 11 shows how CCD works in the case of the leg, applied in the plane perpendicular to the knee joint rotation axis, with rotation angles and directions calculated at each iteration as shown in Eq. 8 and 9.

Considering a joint J situated at the position $p_J \in \mathbb{R}^3$, we apply our segment rotations by defining both the angles θ_J and the axis r_J as following,

$$\begin{cases} \theta_J = \frac{p_A - p_J}{||p_A - p_J||} \cdot \frac{p_G - p_J}{||p_G - p_J||} \\ r_J = \frac{p_A - p_J}{||p_A - p_J||} \times \frac{p_G - p_J}{||p_G - p_J||} \end{cases} . \tag{9}$$

An angle and it's corresponding axis (θ_J, r_J) can then define the quaternion q_J orienting the associated bone segment. The termination criteria of this process depends on the considered error between P_g and P_a, and the maximum number of iterations. As the leg is a simple multi-body mechanism it normally converges after a few iterations, in less than $1ms$. The obtained accuracy is higher in the hip and ankle joints, than in the knee, as the measured hip and ankle positions are explicitly considered in the adjustment. In the general case, according to the experiments done in [40], in a similar context but considering the whole body structure, the RMS accuracy error of CCD, per joint, when partial measurements are used is approximately of 0.03 for a displacement normalized by the height of the person. Finally, Fig. 12 shows the differences between the reconstructed leg with and without this additional procedure. It can be observed, especially in the knee joint, how

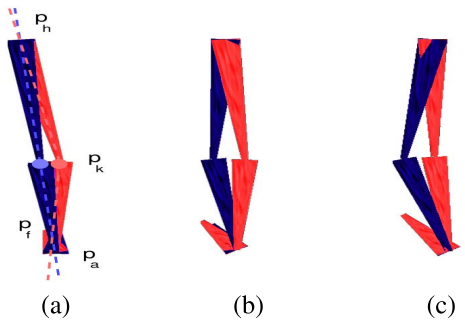

Fig. 12. 3D reconstructed leg before (left) and after applying the IK module (right) from (a) back view and (b) and (c) side views are shown.

applying this kinematic model adjustment helps to preserve the biomechanical characteristics of the lower limb joints' motion.

The RMS error position estimation obtained from our method for the right ankle, right knee and right hip are 1.15m, 1.26m and 1.46m, respectively. As can be seen, RMS error associated with the hip and knee joints are higher than that of the ankle joint. Therefore, if we want to extend this work and generate the entire body (i.e. both upper body and lower body) we need to customise the described Kinematic Model to minimise the error on the upper body joints. In addition, since the subjects were asked to walk on a straight line, Pearson's correlation coefficient (r) and significant difference test results (P) were used to quantify the relationship between the calculated and measured (reference) movements for all joints in the sagittal plane. The correlation between the calculated and the reference was found to have similar trends (right ankle ($r = 0.9426, p < 0.005$), right knee ($r = 0.9612, p < 0.005$), right hip ($r = 0.9682, p < 0.005$), left ankle ($r = 0.9467, p < 0.005$), left knee ($r = 0.9749, p < 0.005$), left hip ($r = 0.9683, p < 0.005$)).

IV. Conclusion

In this paper we have presented a novel low-cost computationally efficient method to accurately reconstruct and monitor the lower limbs. Our system uses body-worn inertial sensors on both left and right thighs, tibias and feet and by utilising a gradient descent-based filter together with the local orientation of each sensor to estimate the associated body segment 3D orientations and 3D positions. In addition, we distinguish between stance and swing phases to obtain drift-free linear velocity from accelerometer signals to calculate accurate 3D position of each foot during the entire gait cycle. Utilising the calculated feet positions along with the estimated orientation of the thighs and tibias, 3D reconstruction of the entire legs was developed via a series of quaternion based geometrical transformations. Finally, it was shown that applying the customised kinematic model increased the accuracy of the system. This system can be extended to reconstruct the entire body and It is envisaged that the proposed method can be used as a lightweight, low-cost system to monitor gait in real-time in non-constrained real-world environments.

References

[1] C. Prakash, K. Gupta, A. Mittal, R. Kumar, and V. Laxmi, "Passive marker based optical system for gait kinematics for lower extremity," *Proc. Comput. Sci.*, vol. 45, pp. 176–185, Dec. 2015.

[2] V. Agostini, M. Knaflitz, L. Antenucci, G. Lisco, L. Gastaldi, and S. Tadano, "Wearable sensors for gait analysis," in *Proc. IEEE Int. Symp. Med. Meas. Appl. (MeMeA)*, May 2015, pp. 146–150.

[3] M. W. Whittle, *Gait Analysis: An Introduction*. London, U.K.: Butterworth, 2014.

[4] E. T. Greenberg, S. Greenberg, and K. Brown-Budde, "Biomechanics and gait analysis for stress fractures," in *Stress Fractures in Athletes*. Switzerland: Springer, 2015, pp. 33–50.

[5] K. Mills, M. A. Hunt, and R. Ferber, "Biomechanical deviations during level walking associated with knee osteoarthritis: A systematic review and meta-analysis," *Arthritis Care Res.*, vol. 65, no. 10, pp. 1643–1665, 2013.

[6] R. W. Kressig *et al.*, "Temporal and spatial features of gait in older adults transitioning to frailty," *Gait Posture*, vol. 20, no. 1, pp. 30–35, 2004.

[7] G. Welch and E. Foxlin, "Motion tracking: No silver bullet, but a respectable arsenal," *IEEE Comput. Graph. Appl.*, vol. 22, no. 6, pp. 24–38, Nov./Dec. 2002.

[8] S. C. Puthenveetil *et al.*, "Comparison of marker-based and marker-less systems for low-cost human motion capture," in *Proc. Int. Design Eng. Tech. Conf. Comput. Inf. Eng. Conf.*, 2013, p. V02BT02A036.

[9] E. Farella, L. Benini, B. Riccò, and A. Acquaviva, "MOCA: A low-power, low-cost motion capture system based on integrated accelerometers," *Adv. Multimedia*, vol. 2007, no. 1, p. 1, 2007.

[10] J. E. Deutsch, M. Borbely, J. Filler, K. Huhn, and P. Guarrera-Bowlby, "Use of a low-cost, commercially available gaming console (Wii) for rehabilitation of an adolescent with cerebral palsy," *Phys. Therapy*, vol. 88, no. 10, pp. 1196–1207, 2008.

[11] M. Windolf, N. Götzen, and M. Morlock, "Systematic accuracy and precision analysis of video motion capturing systems—Exemplified on the *vicon-460* system," *J. Biomech.*, vol. 41, pp. 2776–2780, Aug. 2008.

[12] J.-H. Yoo and M. S. Nixon, "Automated markerless analysis of human gait motion for recognition and classification," *ETRI J.*, vol. 33, no. 2, pp. 259–266, 2011.

[13] A. Castelli, G. Paolini, A. Cereatti, and U. D. Croce, "A 2D markerless gait analysis methodology: Validation on healthy subjects," *Comput. Math. Methods Med.*, vol. 2015, Apr. 2015, Art. no. 186780.

[14] B. F. Mazuquin *et al.*, "Kinematic gait analysis using inertial sensors with subjects after stroke in two different arteries," *J. Phys. Therapy Sci.*, vol. 26, no. 8, pp. 1307–1311, 2014.

[15] W. Tao, T. Liu, R. Zheng, and H. Feng, "Gait analysis using wearable sensors," *Sensors*, vol. 12, no. 12, pp. 2255–2283, 2012.

[16] K. Moran, C. Richter, E. Farrell, E. Mitchell, A. Ahmadi, and N. E. O'Connor, "Detection of running asymmetry using a wearable sensor system," *Proc. Eng.*, vol. 112, pp. 180–183, Dec. 2015.

[17] S. Essid *et al.*, "An advanced virtual dance performance evaluator," in *Proc. IEEE Int. Conf. Acoust., Speech Signal Process. (ICASSP)*, Mar. 2012, pp. 2269–2272.

[18] Z. Zhang, "Microsoft Kinect sensor and its effect," *IEEE Multimedia*, vol. 19, no. 2, pp. 4–10, Feb. 2012.

[19] H. Liu, X. Wei, J. Chai, I. Ha, and T. Rhee, "Realtime human motion control with a small number of inertial sensors," in *Proc. ACM Symp. Interact. 3D Graph. Games*, 2011, pp. 133–140.

[20] A. Ahmadi *et al.*, "Human gait monitoring using body-worn inertial sensors and kinematic modelling," in *Proc. IEEE Conf. SENSORS*, Nov. 2015, pp. 1–4.

[21] J.-P. Tiesel and J. Loviscach, "A mobile low-cost motion capture system based on accelerometers," in *Advances in Visual Computing*. New York, NY, USA: Springer, 2006, pp. 437–446.

[22] D. Roetenberg, H. Luinge, and P. Slycke, "Xsens MVN: Full 6DOF human motion tracking using miniature inertial sensors," Xsens Technol., Enschede, The Netherlands, Tech. Rep., 2009.

[23] D. Vlasic *et al.*, "Practical motion capture in everyday surroundings," *ACM Trans. Graph.*, vol. 26, no. 3, 2007, Art. no. 35.

[24] A. Ahmadi *et al.*, "Toward automatic activity classification and movement assessment during a sports training session," *IEEE Internet Things J.*, vol. 2, no. 1, pp. 23–32, Feb. 2015.

[25] F. Destelle *et al.*, "Low-cost accurate skeleton tracking based on fusion of Kinect and wearable inertial sensors," in *Proc. 22nd Eur. Signal Process. Conf. (EUSIPCO)*, Sep. 2014, pp. 371–375.

[26] F. Destelle *et al.*, "A multi-modal 3D capturing platform for learning and preservation of traditional sports and games," in *Proc. 23rd Annu. ACM Conf. Multimedia*, 2015, pp. 747–748.

[27] S. O. H. Madgwick, A. J. L. Harrison, and R. Vaidyanathan, "Estimation of IMU and MARG orientation using a gradient descent algorithm," in *Proc. IEEE Int. Conf. Rehabil. Robot. (ICORR)*, Jun./Jul. 2011, pp. 1–7.

[28] A. Ahmadi, F. Destelle, D. Monaghan, N. E. O'Connor, C. Richter, and K. Moran, "A framework for comprehensive analysis of a swing in sports using low-cost inertial sensors," in *Proc. IEEE Conf. SENSORS*, Nov. 2014, pp. 2211–2214.

[29] B. Mariani, S. Rochat, C. J. Büla, and K. Aminian, "Heel and toe clearance estimation for gait analysis using wireless inertial sensors," *IEEE Trans. Biomed. Eng.*, vol. 59, no. 11, pp. 3162–3168, Nov. 2012.

[30] A. R. Jimenez, F. Seco, C. Prieto, and J. Guevara, "A comparison of pedestrian dead-reckoning algorithms using a low-cost MEMS IMU," in *Proc. IEEE Int. Symp. Intell. Signal Process. (WISP)*, Aug. 2009, pp. 37–42.

[31] F. Dadashi, B. Mariani, S. Rochat, C. J. Büla, B. Santos-Eggimann, and K. Aminian, "Gait and foot clearance parameters obtained using shoe-worn inertial sensors in a large-population sample of older adults," *Sensors*, vol. 14, no. 1, pp. 443–457, 2013.

[32] X. Yun, E. R. Bachmann, H. Moore, IV, and J. Calusdian, "Self-contained position tracking of human movement using small inertial/magnetic sensor modules," in *Proc. IEEE Int. Conf. Robot. Autom.*, Apr. 2007, pp. 2526–2533.

[33] M. Zoppi, "Effective backward kinematics for an industrial 6R robot," in *Proc. ASME Design Eng. Tech. Conf. Comput. Inf. Eng. Conf. (DETC)*, Montreal, Canada, 2002, pp. 497–503.

[34] X. Wu, L. Ma, Z. Chen, and Y. Gao, "A 12-DOF analytic inverse kinematics solver for human motion control," *J. Inf. Comput. Sci.*, vol. 1, no. 1, pp. 137–141, 2004.

[35] J. Q. Gan, E. Oyama, E. M. Rosales, and H. Hu, "A complete analytical solution to the inverse kinematics of the pioneer 2 robotic arm," *Robotica*, vol. 23, no. 1, pp. 123–129, 2005.

[36] L.-C. T. Wang and C. C. Chen, "A combined optimization method for solving the inverse kinematics problems of mechanical manipulators," *IEEE Trans. Robot. Autom.*, vol. 7, no. 4, pp. 489–499, Aug. 1991.

[37] P. Baerlocher and R. Boulic, "An inverse kinematics architecture enforcing an arbitrary number of strict priority levels," *Vis. Comput., Int. J. Comput. Graph.*, vol. 20, no. 6, pp. 402–417, Aug. 2004.

[38] S. R. Buss and J.-S. Kim, "Selectively damped least squares for inverse kinematics," *J. Graph. Tools*, vol. 10, no. 3, pp. 37–49, 2005.

[39] R. Kulpa, F. Multon, and B. Arnaldi, "Morphology-independent representation of motions for interactive human-like animation," *Comput. Graph. Forum*, vol. 24, no. 3, pp. 343–351, 2005.

[40] L. Unzueta, M. Peinado, R. Boulic, and Á. Suescun, "Full-body performance animation with sequential inverse kinematics," *Graph. Models*, vol. 70, no. 5, pp. 87–104, 2008.

[41] A. Aristidou and J. Lasenby, "FABRIK: A fast, iterative solver for the inverse kinematics problem," *Graph. Models*, vol. 73, no. 5, pp. 243–260, 2011.

Amin Ahmadi received the master's and Ph.D. degrees in microelectronic engineering from Grifth University, Brisbane, Australia, in 2006 and 2010, respectively. He was a Research Scientist with the NICTA Queensland Research Laboratory, Australia, from 2011 to 2013. He joined the Insight Center for Data Analytics, Dublin, Ireland, in 2013. He is currently a Research Fellow involved in a number of European funded projects to develop novel solutions for monitoring and analyzing human movements using wearable inertial sensors and computer vision techniques. His research interests include sensor fusion, machine learning and human motion analysis using wearable inertial sensors for rehabilitation, and sporting activity applications.

François Destelle received the Ph.D. degree in computer graphics from the National Polytechnic Institute of Grenoble, Grenoble, France, in 2010. He was a Post-Doctoral Fellow with the Department of Computer Graphics, LE2I, Dijon, France, in 2011 and was a Research Associate with the Department of Computer Vision, LE2I, in 2012. He is currently a Post-Doctoral Researcher with the Insight Centre for Data Analytics, Dublin City University, Dublin, Ireland, where he is involved with the RePlay project to develop novel solutions for capturing and reconstructing moving athletes in 3D using wearable inertial sensors and computer vision techniques.

Luis Unzueta (M'10) received the M.S. and Ph.D. degrees in mechanical engineering from Tecnun, University of Navarra, Donostia-San Sebastian, Spain, in 2002 and 2009, respectively. He is currently a Researcher of the ITS and Engineering Area of Vicomtech, Donostia-San Sebastian, Spain, where he is involved in research and innovation projects about human detection and understanding, for different kinds of applications, such as natural interaction, sports analysis, and video surveillance. His current research interests include computer vision, motion capture, and human–computer interaction.

David S. Monaghan is currently pursuing the Ph.D. degree in electronic engineering. He is also a Computer Scientist and a Fulbright Scholar. He is also a University Research Fellow and the Team Leader of the Multi-Modal Human Sensing Group at the Insight Centre for Data Analytics, Dublin City University, Ireland. He currently works on smart and connected health applications and the development of home-based rehabilitation systems that use computer gaming technologies He is also passionate about Art/Science projects and has been involved in several high profile national and European Art exhibitions.

Maria Teresa Linaza received the M.S. and Ph.D. degrees in electrical, electronic, and control engineering from the Escuela Superior de Ingenieros Industriales, University of Navarra, Donostia-San Sebastian, Spain, in 1996 and 2001, respectively. She is currently the Head of the eTourism and Cultural Heritage Department of Vicomtech-IK4, Donostia-San Sebastian, Spain. She is also leading the research areas of the Department as well as managing European, national and regional R&D projects.

Kieran Moran received the B.Sc. degree in sport studies and the Ph.D. degree in movement biomechanics from the University of Ulster, Ulster, Northern Ireland, in 1993 and 1997, respectively. Since 1999, he has been with the School of Health and Human Performance, Dublin City University, Dublin, Ireland; promoted to Senior Lecturer in 2009, and currently the Head of the School. He serves on a number of industry research advisory boards and journal editorial advisory boards. His research interests include sensors to monitor movement (physical activity, sport and exercise) in nonlaboratory settings in order to predict, diagnose, and rehabilitate musculoskeletal-based injuries.

Noel E. O'Connor received the Ph.D. degree from Dublin City University, Dublin, Ireland, in 1992. He is currently a Professor with the School of Electronic Engineering, Dublin City University. He has authored over 200 peer-reviewed publications in high prole journals and conferences and has edited six journal special issues. His research interests include multimodal content analysis leveraging mutually complementary sensor data sources, for applications in sports, ambient-assisted living, social digital media, and environmental monitoring. He is a member of the IET. He is an Area Editor for *Signal Processing: Image Communication* (Elsevier) and an Associate Editor for the *Journal of Image and Video Processing* (Springer). He was a recipient of the DCU Presidents Research Award for Science and Engineering in 2010. Also, in 2010, he was a recipient of Enterprise Irelands National Commercialization Award for ICT.